Zygfryd GŁOWACZ*, Jarosław KOZIK*

MATHEMATICAL MODELLING OF SYNCHRONOUS MACHINE POWERED FROM CYCLOCONVERTERS**

SUMMARY

Synchronous machine powered from cycloconverter might be investigated using constant or variable structure methods [4]. There is no mathematical model with constant structure and variable parameters of synchronous machine powered from cycloconverter in the literature. The purpose of this paper is to formulate the mathematical model with variable parameters of synchronous machine powered from 3-pulse cycloconverter.

***Keywords**: synchronous machine, cycloconverter*

MATEMATYCZNE MODELOWANIE MASZYNY SYNCHRONICZNEJ ZASILANEJ Z CYKLOKONWERTORA

Maszyna synchroniczna zasilana z cyklokonwertora może być badana metodami zmiennej lub stałej struktury. W artykule zaproponowano matematyczny model o zmiennych parametrach przy założeniu stałej struktury maszyny synchronicznej i układu zasilającego (cyklokonwertora trójpulsowego). Utworzony model pozwala badać zarówno stany bezawaryjne, jak i awaryjne układu.

***Słowa kluczowe**: maszyna synchroniczna, cyklokonwertor*

1. INTRODUCTION

Discrete-continuous electrical systems with semiconductor converter provide high accuracy, performance rate and watt-hour efficiency but they require precise design, testing and high quality of the work [3]. Cycloconverters (called as well direct AC/AC converters) are used to convert an AC waveform to another AC waveform of a lower frequency and same or a lower amplitude. From practical reasons (reducing of the level of higher harmonics generated) the maximum frequency of an output voltage is assumed to be not lower than half of the frequency of an input voltage. A typical aplications of cycloconverters are: controlling the speed of a traction AC motors, ship propulsion, rolling stands, mine winders, mill drives etc. Cycloconverters are especially useful for controlling the speed of a synchronous motors, which motors have a very confined possibilities of a speed control.

The great care should be taken at the construction and manufacturing stages, because any faults, especially within the steering circuitry may cause serious problems in the electrical system (possible phase-to-phase short circuits). Because of that the cyclonverters should be constantly diagnosed for any failure in their circuitry.

2. THE STRUCTURES OF CYCLOCONVERTERS

There are many various types of cycloconverters, depending on the application, but the most popular and most useful for controlling the speed of drive motors are those with 3-phase input and 3-phase output. They can be further subdivided depending on the number of pulses included in the output voltage waveform. The higher number of pulses the less higher harmonics of voltages and currents generated by the cycloconverter , but as well the higher complication in the structure of a device. And that means the higher cost and lower reliability [6]. The popular structures of 3-phase cycloconverters are presented in the Figures 1 and 2.

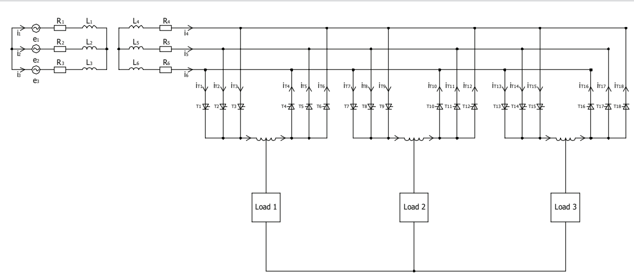

Fig. 1. 3-pulse cycloconverter

Cycloconverters consist of reversible, usually suppressed-half thyristor converters each supplying one phase of the three-phase load. Performing modulation with frequency f_0 of the firing angles of thyristors of both thyristor valves changing in the range from rectifier to inverter work causes the alternating voltage u_0 of frequency f_0 is obtained at the output terminals [5].

Cycloconverters can work with circulating currents or without. While working with circulating currents only one of the antiparallel bridges is in operation at a time. In such a case when current reverses a short dead time can be observed before another antiparallel brigde is fired. During the work with circulating currents both of the antiparallel bridges are working simultaneously and are symetrically controlled according to the formula $\alpha_1 = \pi - \alpha_2$.

The shape of an output voltage waveform depends on the way of changing the realase angles of thysistors. There are two different modes of operation used to control the frequency of output voltage produced by cycloconverter: sinusoidal operation and trapezoidal operation (Figs 3 and 4). In the sinusoidal mode the converters always operate with partial firing angles, whereas in the trapezoidal mode the static converters are operated at their firing limits for as long as possible in the low frequency cycle.

* AGH University of Science and Technology in Cracow, Department of Electrical Machines

** Artykuł uzyskał pozytywne recenzje i był prezentowany podczas Międzynarodowego Sympozjum Maszyn Elektrycznych SME 2006 w Krakowie

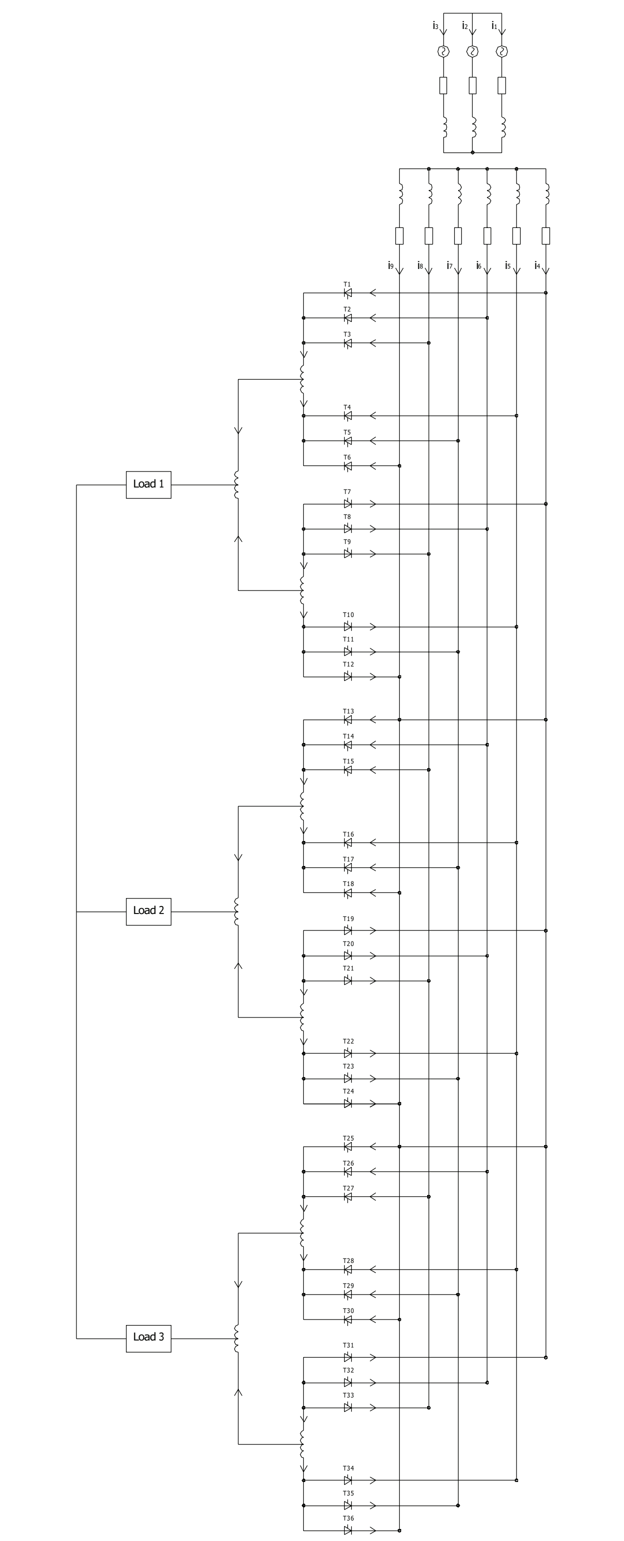

Fig. 2. 6-pulse cycloconverter

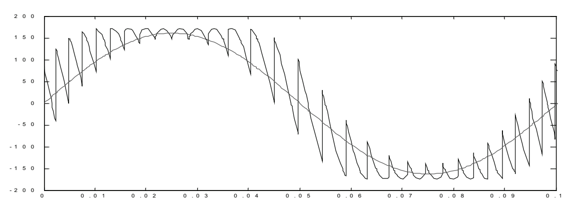

Fig. 3. Output voltage in sinusoidal operation

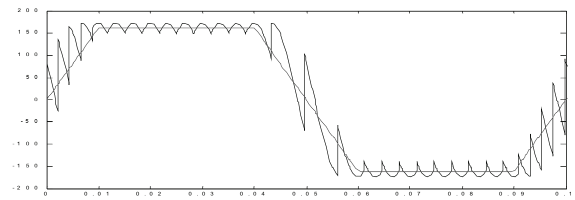

Fig. 4. Output voltage in trapezoidal operation

The constructions of a greater number of pulses may be also encountered.

3. FORMULATION OF THE MATHEMATICAL MODEL OF A 3-PULSE CYCLOCONVERTER SUPPLYING A SYNCHRONOUS MACHINE

The mathematical model of the power circuits has been constructed by using the parametric method of analysis of semiconductor systems. In this method each semiconductor element is approximated by an element with variable parameters. The assumption was made that the value of resistance in conducting state of a semiconductor element is some orders of magnitude lower than in nonconducting state. Thus the created mathematical model of the system is a set of stiff nonlinear differential equations [1].

The mathematical description of system is derived on the following assumptions:

- the magnetic circuit is linear,
- the air-gap is uniform,
- the unipolar flux is neglected,
- the eddy currents in iron are not taken into account,
- the semiconductor elements of the system are approximated by element with variable parameters.

Electrical subsystem of the electromechanical model of a cycloconverter powering a synchronous machine are described by following equations [2]

$$\frac{d}{dt}\left(\mathbf{C}^T \mathbf{L}_g \mathbf{C}\,\mathbf{i}\right) + \mathbf{C}^T \mathbf{R}_g \mathbf{C}\,\mathbf{i} = \mathbf{u} \tag{1}$$

$$\mathbf{i}_g = \mathbf{C}\,\mathbf{i} \tag{2}$$

$$\mathbf{C}^T \mathbf{u}_g = \mathbf{u} \tag{3}$$

where:

- $\mathbf{C}$ – matrix of constraints,
- $\mathbf{L}_g$ – matrix of branch inductions,
- $\mathbf{R}_g$ – matrix of branch resistances,
- $\mathbf{i}_g$ – vector of branch currents,
- $\mathbf{u}_g$ – vector of branch source voltages,
- $\mathbf{i}$ – vector of mesh currents,
- $\mathbf{u}$ – vector of mesh source voltages.

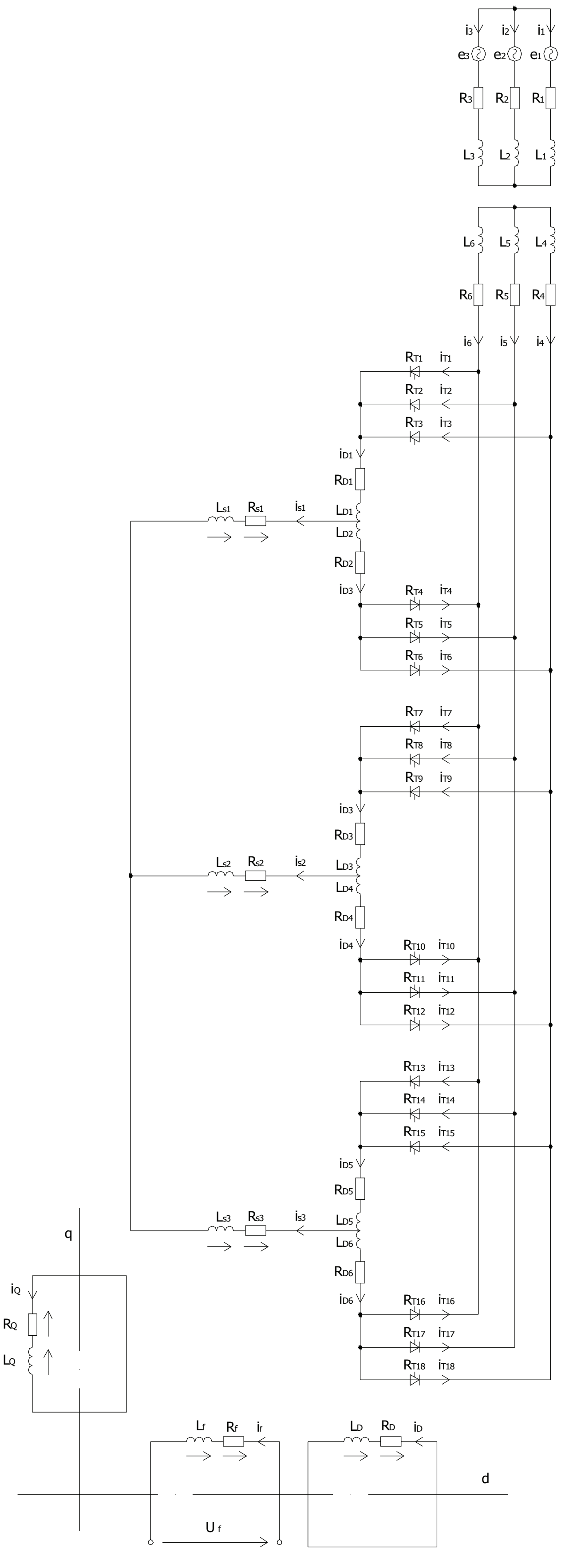

Fig. 5. Electric power circuits of synchronous machine powered from cycloconverter

Mechanical subsystem is described by equations:

$$J_s \frac{d}{dt}\omega_s + D\omega_s = T_e - T_o \tag{4}$$

$$\frac{d}{dt}\varphi_s = \omega_s \tag{5}$$

$$T_e = \frac{1}{2}\mathbf{i}^T \mathbf{C}^T \frac{\partial}{\partial \varphi_s}\left(\mathbf{L}_g\right)\mathbf{Ci} \tag{6}$$

where:

ω_s, φ_s – angular velocity and position of rotor,
T_e, T_o – electromagnetic and load torques,
J_s, D – moment of inertia and suppression factor.

The particular meshes in the model should be chosen in the way, that will allow to separate the differential equations from algebraic ones.

Electric power circuits of synchronous machine powered from 3-pulse cycloconverter are shown in the Figure 5.

The thyristors are represented by two-state resistances determined from the following mathematical model:

$$q_{T\nu}(t+\Delta t) = \begin{cases} 1, \text{ if } & i_{T\nu}(t)\rangle 0 \wedge w_\nu(t)\rangle 0 \wedge q_{T\nu}(t)\rangle 0 \vee \\ & i_{T\nu}(t)\rangle i_h \wedge q_{T\nu}(t)\rangle 0 \vee \\ & u_{T\nu}(t)\rangle 0 \wedge w_\nu(t)\rangle 0 \wedge q_{T\nu}(t) \le 0 \\ 0, & \text{otherwise} \end{cases} \tag{7}$$

$$R_{T\nu}(t) = l(q_{T\nu}, i_{T\nu}) \tag{8}$$

$$u_{T\nu}(t) = R_{T\nu} i_{T\nu} \tag{9}$$

for $\nu \in \{1, 2, \ldots, 18\}$,
where:

$i_{T\nu}$ – current in the branch containing the thyristor,
w_ν – controlling gate signal,
i_h – holding current,
$q_{T\nu}$ – state of the thyristor (conduction or non-conduction),
$u_{T\nu}$ – thyristor voltage,
$T_{T\nu}$ – thyristor resistance.

The matrices and vectors used in the mathematical model of the considered 3-pulse cycloconverter are as follows:

$\mathbf{i}_g = [i_1\ i_2\ i_3\ i_4\ i_5\ i_6\ i_{D1}\ i_{D2}\ i_{D3}\ i_{D4}\ i_{D5}\ i_{D6}\ i_{s1}\ i_{s2}\ i_{s3}\ i_f\ i_D\ i_Q\ i_{T1}\ i_{T2}\ i_{T3}\ i_{T4}\ i_{T5}\ i_{T6}\ i_{T7}\ i_{T8}\ i_{T9}\ i_{T10}\ i_{T11}\ i_{T12}\ i_{T13}\ i_{T14}\ i_{T15}\ i_{T16}\ i_{T17}\ i_{T18}]^T$

$\mathbf{u}_g = [e_1\ e_2\ e_3\ 0\ 0\ 0\ 0\ 0\ 0\ 0\ 0\ 0\ 0\ 0\ 0\ 0\ 0\ 0\ 0\ 0\ 0\ 0\ 0\ 0\ 0\ 0\ 0\ 0\ 0\ 0\ 0\ 0\ 0\ 0\ 0\ 0]^T$

$\mathbf{R}_g = diag([R_1\ R_2\ R_3\ R_4\ R_5\ R_6\ R_{D1}\ R_{D2}\ R_{D3}\ R_{D4}\ R_{D5}\ R_{D6}\ R_{s1}\ R_{s2}\ R_{s3}\ R_f\ R_D\ R_Q\ R_{T1}\ R_{T2}\ R_{T3}\ R_{T4}\ R_{T5}\ R_{T6}\ R_{T7}\ R_{T8}\ R_{T9}\ R_{T10}\ R_{T11}\ R_{T12}\ R_{T13}\ R_{T14}\ R_{T15}\ R_{T16}\ R_{T17}\ R_{T18}])$

$$
\mathbf{C} = \begin{bmatrix}
1 & 0 & 0 & 0 & 0 & 0 & 0 & 0 & 0 & 0 & 0 & 0 & 0 & 0 & 0 & 0 & 0 & 0 & 0 & 0 & 0 & 0 \\
-1 & 1 & 0 & 0 & 0 & 0 & 0 & 0 & 0 & 0 & 0 & 0 & 0 & 0 & 0 & 0 & 0 & 0 & 0 & 0 & 0 & 0 \\
0 & -1 & 0 & 0 & 0 & 0 & 0 & 0 & 0 & 0 & 0 & 0 & 0 & 0 & 0 & 0 & 0 & 0 & 0 & 0 & 0 & 0 \\
0 & 0 & 1 & 0 & 0 & 0 & 0 & 0 & 0 & 0 & 0 & 0 & 0 & 0 & 0 & 0 & 0 & 0 & 0 & 0 & 0 & 0 \\
0 & 0 & -1 & 1 & 0 & 0 & 0 & 0 & 0 & 0 & 0 & 0 & 0 & 0 & 0 & 0 & 0 & 0 & 0 & 0 & 0 & 0 \\
0 & 0 & 0 & -1 & 0 & 0 & 0 & 0 & 0 & 0 & 0 & 0 & 0 & 0 & 0 & 0 & 0 & 0 & 0 & 0 & 0 & 0 \\
0 & 0 & 0 & 0 & 1 & 0 & 0 & 1 & 0 & 0 & 0 & 0 & 0 & 0 & 0 & 0 & 0 & 0 & 0 & 0 & 0 & 0 \\
0 & 0 & 0 & 0 & 1 & 0 & 0 & 0 & 0 & 0 & 0 & 0 & 0 & 0 & 0 & 0 & 0 & 0 & 0 & 0 & 0 & 0 \\
0 & 0 & 0 & 0 & 0 & 1 & 0 & -1 & 1 & 0 & 0 & 0 & 0 & 0 & 0 & 0 & 0 & 0 & 0 & 0 & 0 & 0 \\
0 & 0 & 0 & 0 & 0 & 1 & 0 & 0 & 0 & 0 & 0 & 0 & 0 & 0 & 0 & 0 & 0 & 0 & 0 & 0 & 0 & 0 \\
0 & 0 & 0 & 0 & 0 & 0 & 1 & 0 & -1 & 0 & 0 & 0 & 0 & 0 & 0 & 0 & 0 & 0 & 0 & 0 & 0 & 0 \\
0 & 0 & 0 & 0 & 0 & 0 & 1 & 0 & 0 & 0 & 0 & 0 & 0 & 0 & 0 & 0 & 0 & 0 & 0 & 0 & 0 & 0 \\
0 & 0 & 0 & 0 & 0 & 0 & 0 & 1 & 0 & 0 & 0 & 0 & 0 & 0 & 0 & 0 & 0 & 0 & 0 & 0 & 0 & 0 \\
0 & 0 & 0 & 0 & 0 & 0 & 0 & -1 & 1 & 0 & 0 & 0 & 0 & 0 & 0 & 0 & 0 & 0 & 0 & 0 & 0 & 0 \\
0 & 0 & 0 & 0 & 0 & 0 & 0 & 0 & -1 & 0 & 0 & 0 & 0 & 0 & 0 & 0 & 0 & 0 & 0 & 0 & 0 & 0 \\
0 & 0 & 0 & 0 & 0 & 0 & 0 & 0 & 0 & 1 & 0 & 0 & 0 & 0 & 0 & 0 & 0 & 0 & 0 & 0 & 0 & 0 \\
0 & 0 & 0 & 0 & 0 & 0 & 0 & 0 & 0 & 0 & 1 & 0 & 0 & 0 & 0 & 0 & 0 & 0 & 0 & 0 & 0 & 0 \\
0 & 0 & 0 & 0 & 0 & 0 & 0 & 0 & 0 & 0 & 0 & 1 & 0 & 0 & 0 & 0 & 0 & 0 & 0 & 0 & 0 & 0 \\
0 & 0 & 0 & 0 & 1 & 0 & 0 & 1 & 0 & 0 & 0 & 0 & 1 & 0 & 0 & 0 & 0 & 0 & 0 & 0 & 0 & 0 \\
0 & 0 & 0 & 0 & 0 & 0 & 0 & 0 & 0 & 0 & 0 & 0 & -1 & 1 & 0 & 0 & 0 & 0 & 0 & 0 & 0 & 0 \\
0 & 0 & 0 & 0 & 0 & 0 & 0 & 0 & 0 & 0 & 0 & 0 & 0 & -1 & 0 & 0 & 0 & 0 & 0 & 0 & 0 & 0 \\
0 & 0 & 0 & 0 & 1 & 0 & 0 & 0 & 0 & 0 & 0 & 0 & 1 & 0 & -1 & 0 & 0 & 0 & 0 & 0 & 0 & 0 \\
0 & 0 & 0 & 0 & 0 & 0 & 0 & 0 & 0 & 0 & 0 & 0 & -1 & 1 & 1 & -1 & 0 & 0 & 0 & 0 & 0 & 0 \\
0 & 0 & 0 & 0 & 0 & 0 & 0 & 0 & 0 & 0 & 0 & 0 & 0 & -1 & 0 & 1 & 0 & 0 & 0 & 0 & 0 & 0 \\
0 & 0 & 0 & 0 & 0 & 1 & 0 & -1 & 1 & 0 & 0 & 0 & 0 & 0 & -1 & 0 & 1 & 0 & 0 & 0 & 0 & 0 \\
0 & 0 & 0 & 0 & 0 & 0 & 0 & 0 & 0 & 0 & 0 & 0 & 0 & 0 & 1 & -1 & -1 & 1 & 0 & 0 & 0 & 0 \\
0 & 0 & 0 & 0 & 0 & 0 & 0 & 0 & 0 & 0 & 0 & 0 & 0 & 0 & 0 & 1 & 0 & -1 & 0 & 0 & 0 & 0 \\
0 & 0 & 0 & 0 & 0 & 1 & 0 & 0 & 0 & 0 & 0 & 0 & 0 & 0 & 0 & 0 & 1 & 0 & -1 & 0 & 0 & 0 \\
0 & 0 & 0 & 0 & 0 & 0 & 0 & 0 & 0 & 0 & 0 & 0 & 0 & 0 & 0 & 0 & -1 & 1 & 1 & -1 & 0 & 0 \\
0 & 0 & 0 & 0 & 0 & 0 & 0 & 0 & 0 & 0 & 0 & 0 & 0 & 0 & 0 & 0 & 0 & -1 & 0 & 1 & 0 & 0 \\
0 & 0 & 0 & 0 & 0 & 0 & 1 & 0 & -1 & 0 & 0 & 0 & 0 & 0 & 0 & 0 & 0 & 0 & -1 & 0 & 1 & 0 \\
0 & 0 & 0 & 0 & 0 & 0 & 0 & 0 & 0 & 0 & 0 & 0 & 0 & 0 & 0 & 0 & 0 & 0 & 1 & -1 & -1 & 1 \\
0 & 0 & 0 & 0 & 0 & 0 & 0 & 0 & 0 & 0 & 0 & 0 & 0 & 0 & 0 & 0 & 0 & 0 & 0 & 1 & 0 & -1 \\
0 & 0 & 0 & 1 & 0 & 0 & 1 & 0 & 0 & 0 & 0 & 0 & 0 & 0 & 0 & 0 & 0 & 0 & 0 & 0 & 1 & 0 \\
0 & 0 & 1 & -1 & 0 & 0 & 0 & 0 & 0 & 0 & 0 & 0 & 0 & 0 & 0 & 0 & 0 & 0 & 0 & 0 & -1 & 1 \\
0 & 0 & -1 & 0 & 0 & 0 & 0 & 0 & 0 & 0 & 0 & 0 & 0 & 0 & 0 & 0 & 0 & 0 & 0 & 0 & 0 & -1
\end{bmatrix}
$$

$$
\mathbf{L}_g = \begin{bmatrix}
\begin{matrix}
L_1 & M_{12} & M_{13} & M_{14} & M_{15} & M_{16} \\
M_{12} & L_2 & M_{23} & M_{24} & M_{25} & M_{26} \\
M_{13} & M_{23} & L_3 & M_{34} & M_{35} & M_{36} \\
M_{14} & M_{24} & M_{34} & L_4 & M_{45} & M_{46} \\
M_{15} & M_{25} & M_{35} & M_{45} & L_5 & M_{56} \\
M_{16} & M_{26} & M_{36} & M_{46} & M_{56} & L_6
\end{matrix} & & & & & & & & & & \\
& L_{D1} & & & & & & & & & \\
& & L_{D2} & & & & & & & & \\
& & & L_{D3} & & & & & & & \\
& & & & L_{D4} & & & & & & \\
& & & & & L_{D5} & & & & & \\
& & & & & & L_{D6} & & & & \\
& & & & & & & \begin{matrix}
L_{s1} & M_{s1s2} & M_{s1s3} & M_{s1f} & M_{s1d} & M_{s1q} \\
M_{s1s2} & L_{s2} & M_{s2s3} & M_{s2f} & M_{s2d} & M_{s2q} \\
M_{s1s3} & M_{s2s3} & L_{s3} & M_{s3f} & M_{s3d} & M_{s3q} \\
M_{s1f} & M_{s2f} & M_{s3f} & L_f & M_{fd} & 0 \\
M_{s1d} & M_{s2d} & M_{s3d} & M_{fd} & L_d & 0 \\
M_{s1q} & M_{s2q} & M_{s3q} & 0 & 0 & L_q
\end{matrix} & & & \\
& & & & & & & & 0 & & \\
& & & & & & & & & \ddots & \\
& & & & & & & & & & 0
\end{bmatrix}
$$

For numerical calculations the above model should be modified. The modification is that the matrices of the mesh inductances $\mathbf{C}^T\mathbf{L}_g\mathbf{C}$ and mesh resistances $\mathbf{C}^T\mathbf{R}_g\mathbf{C}$ are divided into matrices of elements included in the inductive and resistive branches. That means the empty elements in the inductance matrix are removed, causing the inductance matrix being reversible.

Assuming:

$$\mathbf{C}^T \mathbf{L}_g \mathbf{C} = \begin{bmatrix} \mathbf{L}_a & \mathbf{0} \\ \mathbf{0} & \mathbf{0} \end{bmatrix} \tag{10}$$

$$\mathbf{C}^T \mathbf{R}_g \mathbf{C} = \begin{bmatrix} \mathbf{R}_a & \mathbf{R}_{ab} \\ \mathbf{R}_{ba} & \mathbf{R}_b \end{bmatrix} \tag{11}$$

$$\mathbf{i} = \begin{bmatrix} \mathbf{i}_a \\ \mathbf{i}_b \end{bmatrix}, \quad \mathbf{u} = \begin{bmatrix} \mathbf{u}_a \\ \mathbf{u}_b \end{bmatrix} \tag{12}$$

$$\boldsymbol{\Psi}_a = \mathbf{L}_a \mathbf{i}_a \tag{13}$$

We can separate differential equations from resistive ones receiving:

$$\frac{d}{dt}(\boldsymbol{\psi}_a) = \\ = \mathbf{u}_a - \left[\mathbf{R}_a \cdot \mathbf{L}_a^{-1} \boldsymbol{\psi}_a + \mathbf{R}_{ab} \cdot \mathbf{R}_b^{-1} \cdot \left(\mathbf{u}_b - \mathbf{R}_{ba} \cdot \mathbf{L}_a^{-1} \boldsymbol{\psi}_a \right) \right] \tag{14}$$

$$\mathbf{i}_a = \mathbf{L}_a^{-1} \boldsymbol{\psi}_a \tag{15}$$

$$\mathbf{i}_b = \mathbf{R}_b^{-1} \cdot \left(\mathbf{u}_b - \mathbf{R}_{ba} \cdot \mathbf{L}_a^{-1} \boldsymbol{\psi}_a \right) \tag{16}$$

Impulse generation subsystem has been described using following equations:

$$u_{ref\mu}(t) = u_m \sin(\omega_{ref}\, t + \alpha_{ref} - (\mu - 1)\frac{2\pi}{3}) \tag{17}$$

for $\mu \in \{1, 2, \ldots, n\}$, $n = 3$

$$u_\nu(t) = u_m \sin(\omega t - (\nu - 1)\frac{2\pi}{3}) \tag{18}$$

$$g_\nu(t) = u_{ref\mu}(t) - u_\nu(t) \tag{19}$$

$$w_\nu(t) = \begin{cases} 1, & \text{if } [g_\nu(t) \cdot g_\nu(t - \Delta t) \langle 0] \wedge [u_\nu(t) \langle u_\nu(t - \Delta t)] \\ 0, & \text{otherwise} \end{cases} \tag{20}$$

for $\nu \in \{1, 2, \ldots, n\}$, $n = 18$,
where:

- $u_{ref\mu}$ – reference voltage,
- u_ν – input voltage,
- g_ν – auxiliary voltage.

4. CONCLUSIONS

The created mathematical model of investigated system is a set of stiff nonlinear differential, logical and algebraic equations. The model equations can be solved with aid of implicit integration methods, which are effective, but in comparison with explicit methods are more time consuming. The use of a matrix of constraints simplifies the construction of a mathematical model and makes its notation clear. But that simplification causes the machine has to be considered in a natural set of coordinates, which fact complicates the numerical calculations and increases the computation time. Applied constant structure method with thyristor in a form of resistive element is competitive in comparison with other methods: the variable structure method with a thyristor model in the form of an ideal switch and the constant structure method with a thyristor model in the form of the series connection of inductive and resistive elements. This fact influences profitably the relation of computation time due to integration methods.

References

[1] Cash J.R.: *A Class of Implicit Runge-Kutta Methods for the Numerical Integration of Stiff Ordinary Differential Equations.* JACM, Vol. 22, No. 4, 1975, 504–511

[2] Głowacz Z.: *Modelling and Simulation of Semiconductor Systems for Diagnostic Purposes.* Proc. of the 7th European Conference on Power Electronics and Applications, Trondheim, Norway, 1997, 2.1001–2.1006

[3] Kaźmierkowski M.P., Tunia H.: *Automatic Control of Converter-Fed Drives.* Elsevier, Amsterdam, Warsaw, PWN 1994

[4] Noga M., Głowacz Z.: *Model matematyczny i algorytm obliczeniowy dla analizy stanów awaryjnych złożonych układów elektromechanicznych.* Rozprawy Elektrotechniczne, t. 35, z. 4, 1989, 965–991

[5] Nowak M., Barlik R.: *Poradnik Inżyniera Energoelektronika.* Warszawa, WNT 1998

[6] Pelley B.R.: *Tyrystorowe przekształtniki i cyklokonwertory.* Warszawa, WNT 1976

Wpłynęło: 26.09.2006

Zygfryd GŁOWACZ

Ukończył studia magisterskie na Wydziale Elektrotechniki Górniczej i Hutniczej w Krakowie w 1973 roku. Pracę doktorską obronił w 1979, a pracę habilitacyjną w 1998 roku. Tematyka badawcza: maszyny elektryczne, układy elektromechaniczne, energoelektronika, informatyka. Obecnie jest zatrudniony na stanowisku profesora nadzwyczajnego w Katedrze Maszyn Elektrycznych AGH. Jest członkiem IEEE od 1996 oraz Sekcji Cybernetyka w Górnictwie KG PAN od 2003 roku.

e-mail: glowacz@agh.edu.pl

Jarosław KOZIK

Ukończył studia na Wydziale Elektrotechniki, Automatyki, Informatyki i Elektroniki Akademii Górniczo-Hutniczej w roku 2003, uzyskując stopień magistra inżyniera. Obecnie pracuje w Katedrze Maszyn Elektrycznych Akademii Górniczo-Hutniczej w Krakowie na stanowisku asystenta. Jego obszarem zainteresowań są maszyny elektryczne, układy energoelektroniczne i mikroprocesorowe układy sterowania.

e-mail: kozik@agh.edu.pl